J|A|C|S
ARTICLES
Published on Web 05/12/2006

Intrachain Electron Transfer in Conducting Oligomers and Polymers: The Mixed Valence Approach

Jean Christophe Lacroix,* Kathleen Isabelle Chane-Ching, Fabrice Maquère, and François Maurel

Contribution from the ITODYS, Université Paris 7-Denis Diderot, CNRS UMR 7086, 1 rue Guy de la Brosse, 75005 Paris, France

Received January 18, 2006; E-mail: lacroix@paris7.jussieu.fr

Abstract: Organic mixed valence compounds consisting of bisdiarylamino charge-bearing units with an oligothiophene bridge and oligothiophene radical cations have been compared using molecular modeling. The study has been performed with oligomers of 1 to 22 thiophene units. These two series of molecules have several properties in common, and intramolecular Single Electron Transfer (SET) in both series can be described within the same theoretical framework. Conducting oligomer radical cations and slightly doped conducting polymers appear as special cases of the vast ensemble of organic mixed valence compounds. Short oligomers are class III, whereas longer oligomers and conducting polymers are class II. Therefore, doped conducting polymers cannot be correctly modeled using oligomers with a short conjugation length. Experimental evidence extracted from the literature confirms these findings. Single electron transfer theories can thus be used when studying interchain and intrachain electron transfer in slightly doped conducting polymers and in materials consisting of short oligomers. This makes it possible to extract from the UV−vis−near-IR spectra the electron-transfer constant rate along or between the π-conjugated chain. The main differences among inorganic, organic, and conducting oligomer or polymer mixed valence compounds lies in the H_{ab} and λ values associated with these different series. Inorganic mixed valence compounds have small H_{ab} and λ values; organic mixed valence compounds have large H_{ab} and λ values, whereas conducting oligomers and polymers have large H_{ab} but small λ values. This induces charge delocalization to occur for systems larger than those of inorganic and nitrogen-centered organic mixed valence compounds.

Introduction:

Π-Conjugated oligomers and polymers attract considerable attention as functional materials in plastic electronics, and a variety of (opto)electronic devices, such as light-emitting diodes, field-effect transistors, solar cells, and electrochromic devices, have been designed.[1] They are also proposed as molecular wires in molecular electronic devices.[2] Both fields use some kind of charge transfer. Therefore the nature of the charge carriers and the description of charge transfer in these extended π-conjugated systems are of primary importance.

In their neutral form these materials are semiconductors with a band gap in the range 1.5−3.5 eV. Heterogeneous single electron transfer (SET) yields a radical cation (anion) in which the charge can move along the π-conjugated chains. These radical cations (anions) are designated as polarons (by analogy with condensed matter physics terminology: a positive polaron is defined as a radical cation associated with a local geometry relaxation[3]). They exhibit UV−vis near-IR absorptions at lower energy than their neutral form. In a one-electron description of the radical cation, heterogeneous single electron transfer generates, therefore, new electronic states within the $\pi \pm \pi^*$ band gap of the polymer. A singly occupied level is generated above the valence band in the $\pi \pm \pi^*$ band gap, and an empty level appears below the conduction band. Initially, the positive polaron was characterized as exhibiting three allowed electronic absorptions associated with a transition from the top of the valence band to the singly occupied polaron level, one between the two polaron levels, and a transition from the occupied polaron level to the conduction band.[3]

Oligomers with a well defined conjugation length have been the subject of many studies as model compounds for polymers, and oxidation experiments have been widely reported.[4] Such studies have to some extent challenged the initial description. Indeed, only two subgap electronic absorptions for oligothiophene radical cations have been observed. In recent years various experimental and theoretical studies have provided a detailed and coherent insight into the characteristics of the first oxidation states of oligothiophenes with a limited number of rings.[4−15] In the first oxidation wave, a radical cation is formed.

(1) *Handbook of Organic Conductive Molecules and Polymers*; Nalwa, H. S., Ed.; Wiley: New York, 1997; Vols. 1−4.
(2) Aviram, A. *J. Am. Chem. Soc.* **1988**, *110*, 5687.
(3) Bredas, J. L.; Street, G. B. *Acc. Chem. Res.* **1985**, *18*, 309.
(4) (a) van Haare, J. A. E. H.; Havinga, E. E.; van Dongen, J. L. J.; Janssen, R. A. J.; Cornil, J.; Brédas, J. L. *Chem.—Eur. J.* **1998**, *4*, 1509. (b) van Haare, J. A. E. H.; Groenendaal, L.; Havinga, E. E.; Janssen, R. A. J.; Meijer, E. W. *Angew. Chem., Int. Ed. Engl.* **1996**, *35*, 638.
(5) (a) Fichou, D.; Xu, B.; Horowitz, G.; Garnier, F. *Synth. Met.* **1991**, *41*, 463. (b) Fichou, D.; Horowitz, G.; Garnier, F. *Synth. Met.* **1990**, *39*, 125.
(6) (a) Hill, M. G.; Mann, K. R.; Miller, L. L.; Penneau, J.-F. *J. Am. Chem. Soc.* **1992**, *114*, 2728. (b) Hill, M. G.; Penneau, J.-F.; Zinger, B.; Mann, K. R.; Miller, L. L. *Chem. Mater.* **1992**, *4*, 1106.

10.1021/ja060390a CCC: $33.50

It exhibits an ESR signal and two subgap electronic absorptions. The first oxidation potential in dilute solution and the optical transition energies of neutral and radical-cation oligomers decrease with chain length and exhibit an almost linear relationship with the inverse number of thiophene rings ($1/n$). Molecular modeling at various levels reveals that a geometry deformation of the aromatic rings occurs in the radical cation to a semiquinoid structure.[16−21] The spatial extension of this deformation, which is located at the center of the chain, is estimated to be five units or less.

Surprisingly, polaron intrachain transfer has not been the focus of many studies. This probably stems from the initial hope of using such materials in macroscopic or micrometric devices in which interchain or even intergrain electron transfer has been recognized as the limiting step of transport properties. However, with emerging nanosciences and nanotechnologies, the description of intrachain electron transfer in π-conjugated polymers will be of crucial importance for the design of efficient molecular electronic devices. Since most of the devices in plastic electronics and molecular electronics use low charge-carrier concentration or single electron transfer, it is likely that radical cations (polarons) are involved in the transport properties of these devices instead of dications (bipolarons) which are formed at higher doping levels.

In the study of intramolecular ET, symmetrical mixed valence (MV) systems are especially valuable; these are systems that contain two charge-bearing units (M) in different oxidation states (M^n and M^{n+1}) attached symmetrically to a bridge.[22,23] These constitute the most simple electron-transfer systems. Simple inorganic derivatives were first used in order to study basic aspects of ET theories.[24−27] However, since the end of the 1990s it has become evident that compounds with organic charge-bearing units fit into the Robin−Day, Hush intervalence compound framework.[28,29] Therefore, the synthesis and characterization of purely organic MV species have been reported, and such systems are receiving increasing attention because of their use in organic electronic material.[30−34]

In 1967, Robin and Day[28] classified mixed valence compounds with two redox centers into three categories according to the relative magnitude of the electronic interaction (H_{ab}) between the M groups and the reorganization energy (λ): class I, complete valence trapping (negligible electronic coupling between the two redox sites, $H_{ab} = 0$); class II, valence trapping (weak electronic coupling, $2H_{ab} < \lambda$); and class III, delocalized valency (strong electronic coupling, $2H_{ab} > \lambda$).

In class II MV compounds, the equilibrium (intramolecular and solvent) configurations differ at the two sites, and consequently, the two sites are not equivalent. Because electron motion is much faster than nuclear motion, energy conservation requires that, prior to the actual electron transfer, the nuclear configurations of the molecule and the surrounding medium adjust from their equilibrium values to an intermediate configuration in which there is no energy change when the electron transfer between the two sites occurs. As a consequence, there is a barrier for intramolecular single-electron transfer in class II compounds but not in class III compounds

A very important feature of the class II and class III MV complexes is the appearance in the visible or the near-infrared region of an absorption band (E_{op}) called the intervalence transfer or charge-transfer (CT) band, which cannot be attributed to the system subunits or to the bridging ligands (Figure 1). This CT band makes it possible to estimate the two basic parameters, that is, the electronic coupling H_{ab} and the reorganization energy λ that, in the semiclassical Marcus−Hush model, determine the rate constant of the self-exchange electron-transfer process.[35]

For class II systems, the following equation holds

$$E_{op} = h\nu_{max} = \lambda = \lambda_{in} + \lambda_{out}$$

where λ_{in} stands for the internal reorganization energy and λ_{out} stands for the solvent and surrounding reorganization energy, regardless of the degree of delocalization. Note that strong solvent effects are observed in class II MV compounds through the λ_{out} impact on E_{op}. The intensity of the CT transition is related to the electronic coupling element H_{ab}:

$$H_{ab} = 0.0206(\nu_{max}\epsilon_{max}\nu_{1/2})^{1/2}/R$$

where R (in Å) is the effective distance between the donor and acceptor sites (diabatic states), ϵ_{max} (in M^{-1} cm^{-1}) the molar

(7) (a) Bäuerle, P.; Segelbacher, U.; Maier, A.; Mehring, M. *J. Am. Chem. Soc.* **1993**, *115*, 10217. (b) Bäuerle, P.; Segelbacher, U.; Gaudl, K.-U.; Huttenlocher, D.; Mehring, M. *Angew. Chem., Int. Ed. Engl.* **1993**, *32*, 76. (c) Bäuerle, P. *Adv. Mater.* **1992**, *4*, 102.
(8) (a) Audebert, P.; Catel, J. M.; Le Coustumer, G.; Duchenet, V.; Hapiot, P. *J. Phys. Chem. B* **1995**, *99*, 11923. (b) Andrieux, C. P.; Hapiot, P.; Audebert, P.; Guyard, L.; Nguyen Dinh An, M.; Groenendaal, L.; Meijer, E. W. *Chem. Mater.* **1997**, *9*, 723.
(9) (a) Graf, D. D.; Campbell, J. P.; Miller, L. L.; Mann, K. R. *J. Am. Chem. Soc.* **1996**, *118*, 5480. (b) Graf, D. D.; Duan, R. G.; Campbell, J. P.; Miller, L. L.; Mann, K. R. *J. Am. Chem. Soc.* **1997**, *119*, 5888. (c) Yu, Y.; Gunic, E.; Zinger, B.; Miller, L. L. *J. Am. Chem. Soc.* **1996**, *118*, 1013.
(10) (a) Guay, J.; Kasai, P.; Diaz, A. F.; Wu, R.; Tour, J. M.; Dao, L. H. *Chem. Mater.* **1992**, *4*, 1097. (b) Guay, J.; Diaz, A. F.; Wu, R.; Tour, J. M.; Dao, L. H. *Chem. Mater.* **1992**, *4*, 254.
(11) (a) Emmi, S. S.; D'Angelantonio, M.; Beggiato, G.; Poggi, G.; Geri, A.; Pietropaolo, D.; Zotti, G. *Radiation Physics and Chemistry* **1999**, *54*, 263. (b) Emmi, S. S.; Poggi, G.; D'Angelantonio, M.; Russo, M.; Favaretto, L. *Radiation Physics and Chemistry* **2003**, *67*, 251.
(12) Alberti, A.; Ballarin, B.; Guerra, M.; Macciantelli, D.; Mucci, A.; Parenti, F.; Schenetti, L.; Seeber, R.; Zanardi, C. *ChemPhysChem* **2003**, *4*, 1216.
(13) Domagala, W.; Lapkowski, M.; Guillerez, S.; Bidan, G. *Electrochim. Acta* **2003**, *48*, 2379.
(14) Apperloo, J.; Janssen, R. A. J.; Malenfant, P. R. L.; Groenendaal, L.; Frechet, J. M. J. *J. Am. Chem. Soc.* **2000**, *122*, 7042.
(15) Nishinaga, T.; Wakamiya, A.; Yamazaki, D.; Komatsu, K. *J. Am. Chem. Soc.* **2004**, *126*, 3163.
(16) Cornil, J.; Bredas, J. L. *Adv. Mater.* **1995**, *7*, 295.
(17) Cornil, J.; Beljonne, D.; Brédas, J. L. *J. Chem. Phys.* **1995**, *103*, 842.
(18) Moro, G.; Scalmani, G.; Cosentino, U.; Pitea, D. *Synth. Met.* **2000**, *108*, 165.
(19) Brocks, G. *Synth. Met.* **1999**, *102*, 914.
(20) (a) Geskin, V. M.; Dkhissi, A.; Brédas, J. L. *Int. J. Quantum Chem.* **2003**, *91*, 350. (b) Dkhissi, A.; Beljonne, D.; Lazzaroni, R.; Louwet, F.; Groenendaal, L.; Bredas, J. L. *Int. J. Quantum Chem.* **2003**, *91*, 517.
(21) (a) Lacroix, J. C.; Maurel, F.; Lacaze, P. C. *J. Am. Chem. Soc.* **2001**, 123, 1989. (b) Lacroix, J. C.; Valente, R. J.; Maurel, F.; Lacaze, P. C. *Chem.—Eur. J.* **1998**, *4*, 1667.
(22) Brown, D. M. In *Mixed Valence Compounds*; Reidel, D., Ed.; Kluwer Academic Publishers: Dordrecht, The Netherlands, 1980.
(23) *Mixed Valence Systems: Applications in Chemistry, Physics and Biology*; Prassides, K., Ed.; NATO ASI Series 343; Kluwer Academic Publishers: Dordrecht, The Netherlands, 1990.
(24) Demadis, K. D.; Hartshorn, C. M.; Meyer, T. J. *Chem. Rev.* **2001**, *101*, 2655.
(25) Crutchley, R. J. *Adv. Inorg. Chem.* **1994**, *41*, 273.
(26) Creutz, C. *Prog. Inorg. Chem.* **1983**, *30*, 1.
(27) Launay, J. P. *Chem. Soc. Rev.* **2001**, *30*, 386.
(28) Robin, M. B.; Day, P. *Adv. Inorg. Radiochem.* **1967**, *10*, 247.
(29) Hush, N. S. *Prog. Inorg. Chem.* **1967**, *8*, 391.
(30) Lambert, C.; Nöll, G. *J. Am. Chem. Soc.* **1999**, *121*, 273.
(31) Nelsen, S. F.; Ismagilov, R. F.; Trieber, D. A. *Science* **1997**, *278*, 846.
(32) Nelsen, S. F. *Chem.—Eur. J.* **2000**, *6*, 581.
(33) Evans, C. E. B.; Naklicki, M. L.; Rezvani, A. R.; White, C. A.; Kondratiev, V. V.; Crutchley, R. J. *J. Am. Chem. Soc.* **1998**, *120*, 13096.
(34) Demadis, K. D.; El-Samanody, E.-S.; Coia, G. M.; Meyer, T. J. *J. Am. Chem. Soc.* **1999**, *121*, 535.
(35) (a) Marcus, R. A. *Discuss. Faraday Soc.* **1960**, 29, 21. (b) Marcus, R. A.; Sutin, N. *Comments Inorg. Chem.* **1986**, *5*, 119.

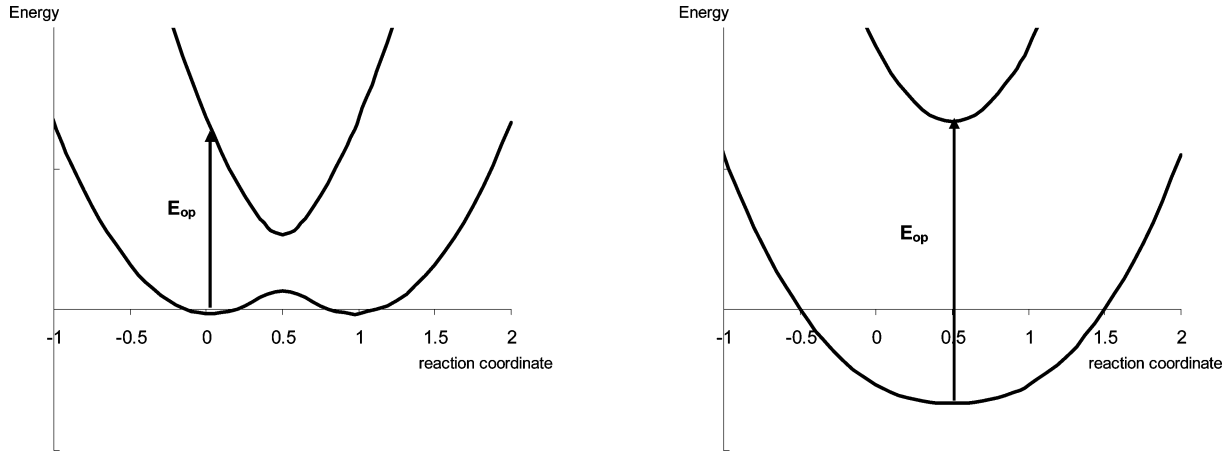

Figure 1. Energy-coordinate diagrams for adiabatic states in class II and class III mixed valence compounds.

extinction coefficient, and $\nu_{1/2}$ the full width at half-maximum (with H_{ab}, ν_{max}, and $\nu_{1/2}$ in cm^{-1}).

The Hush model remains the preferred method for analyzing CT spectra because of its simplicity and ease of application..

For class III compounds the following equation holds

$$E_{op} = 2H_{ab}$$

The reorganization energy cannot be estimated from the optical spectra, but H_{ab} can be directly measured. Note also that the optical transition no longer involves charge transfer and is therefore not accompanied by a net dipole moment change and thus shows no solvent dependence. Instead, the optical absorption involves transitions between delocalized orbitals of the systems.

Many aspects of mixed valence compounds have been studied in great detail (class II−III transition regime,[24,32,36] shape, and truncation of the intervalence band,[24,32,36] increasingly complex models including two to four states,[36] the effect of bridge redox state on electron transfer,[36,37] topological effects via quantum interference,[38] length dependence of intramolecular electron transfer,[39,40] solvent and ion pairing effects[41]) and will be described if needed within the different parts of this paper.

In this work we will focus on the differences and the properties in common between organic mixed valence compounds consisting of bisdiarylamino charge-bearing units and conjugated bridges, recently described by Lambert and Nöll,[30] and oligothiophene radical cations (Scheme 1). The former are considered as the prototype for testing SET theories; in the latter intrachain electron transfer is poorly described and does not use intramolecular SET theories. To have very similar molecular structures, the organic mixed valence compounds will have an oligothiophene bridge (instead of the oligophenyl bridge in Lambert and Nöll's study).[30] Molecular modeling will be the main tool since it has proved to give strong insights in ET studies on organic MV compounds.[42,43] Furthermore, we shall consider

Scheme 1. Mixed Valence Compounds and Oligothiophene Radical Cations to Be Compared

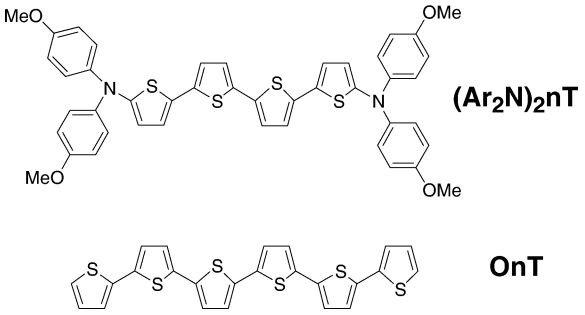

various oligomer lengths from 1 to 22 thiophenes in order to cover the full scale from short to intermediate and very long oligomers. In doing so we want to give enough space for intramolecular electron transfer to be unaffected by boundary effects and we hope to get some insights into the general belief that conducting polymers can be correctly modeled using oligomers with a well-defined conjugation length.

Modeling Strategy. Many studies have used quantum chemistry in order to study electron transfer in organic mixed valence compounds.[38,39,42−44] From the Hückel model[38] to TDDFT methods within vibronic coupling[42] studies most quantum chemical methods have been used to describe various aspects of intramolecular electron transfer. Earlier studies were performed within the very approximate one-electron Extended Hückel model and proved useful for the qualitative determination of H_{ab}, in the study of topological effects via quantum interference and in the bridge length dependence of intramolecular electron transfer.[38] Semiempirical,[43,44] ab initio Hartree−Fock[39] and DFT methods[42] have also been used. However, DFT methods suffer from an intrinsic tendency to enhance the metallike behavior of large bridging molecules[45] or oligothiophenes[18−20] and are therefore not appropriate for calculating the geometry of the species under study.

Owing to the size of the molecule modeled in this study (22T or (bisdiarylamino) with six thiophenes in the bridge) we have

(36) Brunschwig, B. S.; Creutz, C.; Sutin, N. *Chem. Soc. Rev.* **2002**, *31*, 168.
(37) Nelsen, S. F.; Ismagilov, R. F.; Powell, D. R. *J. Am. Chem. Soc.* **1998**, *120*, 1924.
(38) Patoux, C.; Coudret, C.; Launay, J. P.; Joachim, C.; Gourdon, A. *Inorg. Chem.* **1997**, *36*, 5037.
(39) Pati, R.; Karna, S. P. *Chem. Phys. Lett.* **2002**, *351*, 302.
(40) Davis, W. B.; Ratner, M. A.; Wasielewski, M. R. *J. Am. Chem. Soc.* **2001**, *123*, 7877.
(41) (a) Nelsen, S. F.; Ismagilov, R. F. *J. Phys. Chem.* **1999**, *103*, 5373. (b) Nelsen, S. F.; Trieber D. A.; Ismagilov, R. F.; Teki, Y. *J. Am. Chem. Soc.* **2001**, *123*, 5684.
(42) Coropceanu, V.; Malagoli, M.; André, J. M.; Brédas, J. L. *J. Am. Chem. Soc.* **2002**, *124*, 10519.
(43) Pourtois, G.; Beljonne, D.; Cornil, J.; Ratner, M. A.; Brédas, J. L. *J. Am. Chem. Soc.* **2002**, *124*, 4436.
(44) Nelsen, S. F.; Tran, H. Q.; Nagy, M. A. *J. Am. Chem. Soc.* **1998**, *120*, 298.
(45) Suhai, S. *Phys. Rev. B.* **1995**, *51*, 16553.

Table 1. Comparison among TDDFT//B3LYP6-31G*, PM3CI// UAM1, and Experimental Values for the First and Second Optical Transition of Oligothiophenes of Various Lengths

	first transition in eV			second transition in eV		
compound	TDDFT// B3LYP6-31G*	PM3CI// UAM1	expmt	TDDFT// B3LYP6-31G*	PM3CI// UAM1	expmt
3T	1.61	1.19	1.32[a]	2.59	2.12	2.00[a] 2.25[b] 2.28[c]
4T	1.28	1.00	1.05[a]	2.2	1.86	1.79[a] 1.91[c]
6T	0.9	0.88	0.84[b]	1.85	1.69	1.59[b] 1.57[c]
9T	0.66	0.68	0.67[b]	1.34	1.44	1.46[b]
12T	0.58	0.63	0.5 [b]	1.23	1.38	1.42[b]

[a] Reference 4. [b] Reference 7. [c] Reference 15.

used AM1-UHF for geometry optimization. The optimized geometry and charge distribution calculated at the AM1-UHF level is known to be consistent with the formation of a localized charge defect characterized by a semiquinoid structural distortion in the oligothiophene radical cation.

In recent years tremendous progress has been made in excited-state calculations. On the basis of the AM1-UHF geometry, TDDFT calculations in the oligothiophene series were performed and compared with configuration interaction using the PM3 Hamiltonian (PM3/CI) with an active space of 40 molecular orbitals. The transition energies calculated with these two methods are reported in Table 1 and are found to be in good agreement with experimental values (when available). Transition energies and oscillator strengths have therefore been determined by means of PM3/CI calculations for all compounds studied. PM3/CI instead of ZINDO/CIS, which gives good agreement between experimental and computed optical absorption energies,[46] has been used because it makes it possible to evaluate charge distribution in the first exited state (through the root=n keywords) and qualitatively describe solvent effects as depicted below.

Such molecular modeling will make it possible to obtain the geometries of the radical cations studied. Plots of the charge difference between the neutral and corresponding radical cations will make it possible to evaluate where the charge is prior to photon absorption, and plots of the charge difference between the first exited state (vertical excitation) and the ground state of the radical cation will indicate where the charge goes upon excitation in the charge-transfer band. Furthermore, calculated E_{op} will give an evaluation of H_{ab} or λ_{in} for each MV compound.

Quantum modeling of solvation effects within continuum approaches, such as those developed by Thrular et al.,[47] can give the free energies of solvation of molecules and ions. Solvent effects on optical properties were computed by running PM3/CI=40 in SM5CR[48] on SM5C/UAM1-optimized geometries (the geometry is optimized in the liquid phase). To the best of our knowledge this procedure has not been previously used to evaluate solvent effects on MV compounds. The results obtained are therefore qualitative and need to be checked against reference compounds for quantitative use.

Finally we want to stress that the precise calculation of optical properties is not attempted in this study since our main concern is to compare intramolecular electron transfer between two series of molecules, the first consisting of organic MV compounds in which the usual electron transfer theories are widely used and the second consisting of oligothiophenes in which usual intramolecular electron transfer theories are merely used. Whether the semiempirical calculations we employ here are good enough to fit experimental values for a given compound and whether these calculations make it possible to compare the optical properties of the two series under study are obvious separate questions. All calculations were performed using the Ampac 6.7 package[49] or the Gaussian 98.[50]

Results

I. (Bisdiarylamino)oligothiophene. Gas-Phase Geometry. Figure 2 shows the gas-phase bond length alternation of several $(Ar_2N)_2$nT in their neutral and singly oxidized states. Neutral systems have symmetrical geometries with equal N−C_α bond lengths and bond length alternation in which the C_α−C_β bonds are short, whereas the C_β−C_β and C_α−C_α' bonds are long. The geometries of the corresponding radical cations are bridge-length-dependent.

For short $(Ar_2N)_2$nT with bridges consisting of one or two thiophene units (Figure 2a), the calculated geometries of the radical cations are symmetrical, but the bond length alternation is reversed, and the N−C_α bond is shorter than that in the neutral molecule (1.36 Å versus 1.41 Å). In a mixed valence description such calculated geometries are indicative of class III compounds with fully delocalized electrons and $2H_{ab} > \lambda$.

For $(Ar_2N)_2$nT with longer bridges ($n > 3$), the calculated geometries are no longer symmetrical and are consistent with the formation of a localized charge defect characterized by a semiquinoid structural distortion (Figure 2b). This defect is situated on one side of the molecule, and consequently one of the N−C_α bonds is short, whereas the other is close to that calculated for the neutral compound. However, the spatial extension of this defect is not restricted to this bond and extends onto the oligothiophene bridge. It can be estimated to be between three and four thiophene units as judged through the bond alternation pattern presented in Figure 2. For $(Ar_2N)_2$nT with bridges longer than four thiophene units the localized charge defect seems to be similar for all the calculated structures. In a mixed valence description such geometries are indicative of class II compounds with the appearance of two minima on the adiabatic potential surface, with an activation barrier separating these two minima, and electron transfer being thermally activated. Such behavior is fully in line with what is expected, since when the bridge length increases H_{ab} decreases and for some bridge length $2H_{ab}$ will become smaller than λ, resulting in a transition between class III and class II. Bisdiarylamino-biphenyl is considered as a class II mixed valence compound, and further increase in bridge length in the molecule studied by Lambert and Noll[30,42] results in slower intramolecular electron transfer as a consequence of the progressive decrease in H_{ab}.

Charge Distribution in Ground State. Figure 3 shows, for several $(Ar_2N)_2$nT, the charge difference between the neutral

(46) Hutchison, G. R.; Ratner, M. A.; Marks, T. J. *J. Phys. Chem. A* **2002**, *106*, 10596.
(47) Cramer, C. J.; Truhlar, D. G. *Science* **1992**, *256*, 213.
(48) (a) Hawkins, G. D.; Cramer, C. J.; Reuhlar D. G. *J. Phys Chem. B* **1998**, *102*, 3257. (b) Dolney, D. M.; Hawkins, G. D.; Winget, P.; Liotard, D. A.; Cramer, C. J.; Truhlar, D. G. *J. Comput. Chem.* **2000**, *21*, 340.
(49) Ampac 6.7 ed. Semichem: Shawnee, KS, 1997.
(50) Frisch et al. *Gaussian 98*, revision A.1; Gaussian, Inc.: Pittsburgh, PA, 1998.

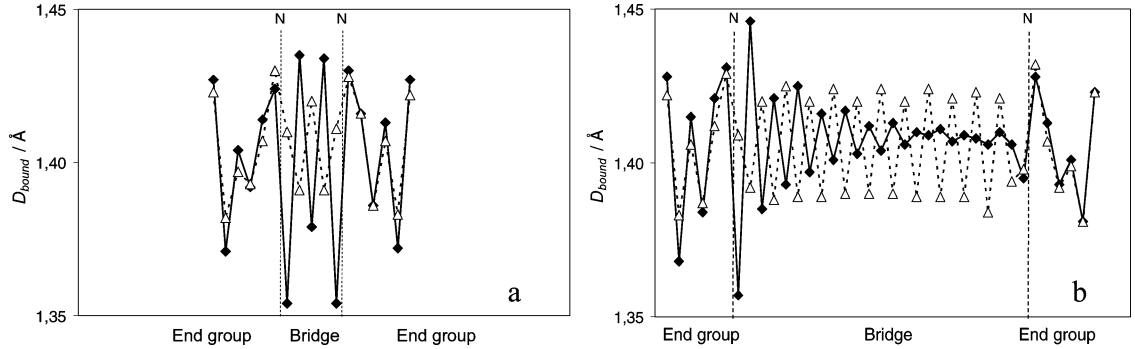

Figure 2. Bond lengths in neutral $(Ar_2N)_2nT$ (△) and of their corresponding radical-cations (◆): (a) $(Ar_2N)_2T$; (b) $(Ar_2N)_26T$.

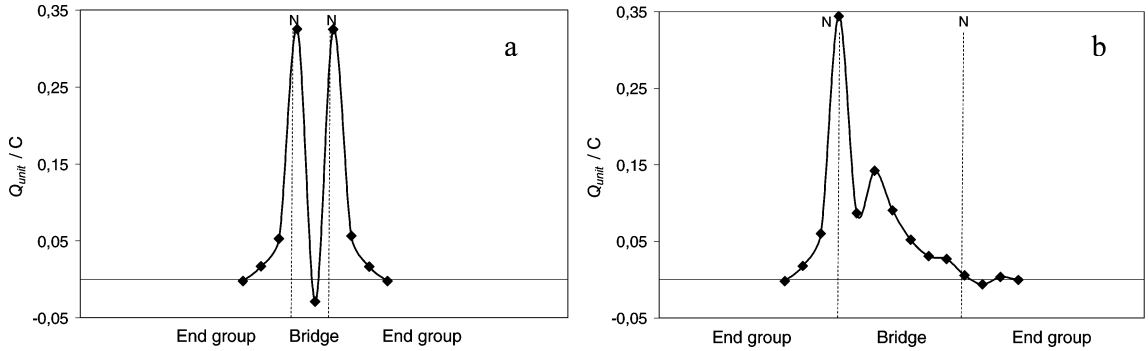

Figure 3. Charge difference between $(Ar_2N)_2nT$ radical cation and neutral $(Ar_2N)_2nT$: (a) $(Ar_2N)_2T$; (b) $(Ar_2N)_26T$.

Table 2. PM3CI//UAM1-Calculated Transition Energies, Oscillator Strength, and Main CI Coefficients in the Excited State for $(Ar_2N)_2nT$ Radical Cations

compound	E_{op} [eV]	oscillator strength	main CI coefficients of the excited state
$(Ar_2N)_21T$	1.20	0.015	30% HOMO → SOMO 51% SOMO → LUMO
$(Ar_2N)_22T$	0.92	0.018	45% HOMO → SOMO 41% SOMO → LUMO
$(Ar_2N)_24T$	0.70	0.334	63% HOMO → SOMO 14% SOMO → LUMO
$(Ar_2N)_26T$	0.78	0.377	20% HOMO → SOMO 34% HOMO-1 → SOMO 12% SOMO → LUMO

and the corresponding radical cation. These charges are compiled on terminal methyl, oxygen atom, phenyl units, N atoms, and thiophene units. This rather empirical description makes it possible to represent qualitatively where the charge is and the extent of charge delocalization in the molecule prior to photon absorption.

As expected for short $(Ar_2N)_2nT$ with one or two thiophene bridges (Figure 3a), the calculated charge distribution is symmetrical with both N atoms bearing the same overall charge, which confirms the class III character of these systems in the gas phase.

For $(Ar_2N)_2nT$ with longer bridges, the charge distributions are no longer symmetrical and are localized on one side of the molecule (Figure 3b). The charge defect extends mainly over the first units of the oligothiophene bridge. For $(Ar_2N)_2nT$ with bridges longer than four thiophene units the spatial extension of the charge defect is bridge-length-independent (not shown).

Optical Properties. The UV−vis−near-IR spectra of the molecules have been calculated at the PM3(CI=40)//UAM1 level. Table 2 gives the transition energies, intensities, and main CI expansion coefficients of the first excited state for several $(Ar_2N)_2nT$ radical cations.

We will first focus on bisdiarylaminothiophene and bisdiarylaminobithiophene radical cations which can be considered as class III systems in the gas phase. The lowest energy transitions are at 1.20 and 0.92 eV, respectively, which means that $H_{ab} = E_{op}/2$ is 0.6 and 0.46 eV for these two molecules. These lowest energy absorptions are not very intense and essentially correspond to transitions between the SOMO and the LUMO and between the HOMO and the SOMO. Apart from these absorptions, at higher energy the spectra are dominated by an intense band at 2.10 and 1.93 eV. Like the lowest energy absorption, these absorptions correspond to a transition between the SOMO and the LUMO and between the HOMO and the SOMO with reversed main CI expansion coefficients of the excited states. These MOs are delocalized over the bridge and the nitrogen atoms; therefore, such transitions can be seen as $\pi-\pi^*$ transitions and are not associated with a charge-transfer process.

As examples of longer MV compounds, the first optical transition energies, intensities, and main CI expansion coefficients of the exited states for $(Ar_2N)_24T$ and $(Ar_2N)_26T$ radical cations are reported in Table 2. E_{op} no longer decreases as in the case of class III compounds but increases slightly with the bridge length. According to Hush theory, localization occurs when $\lambda/2$ is greater than H_{ab}, so for these compounds we have $E_{op} = \lambda_{in}$. Transition dipole moments are high and directed along the N−N axis of the molecule but do not depend on bridge length. The orbitals involved in the one-electron transition describing the first excited state are depicted in Figure 4 for bisdiarylaminoquaterthiophene and clearly suggest that this transition is associated with a charge transfer from one part of the molecule toward the side of the molecule bearing the charge defect in the ground state. The calculations also indicate that

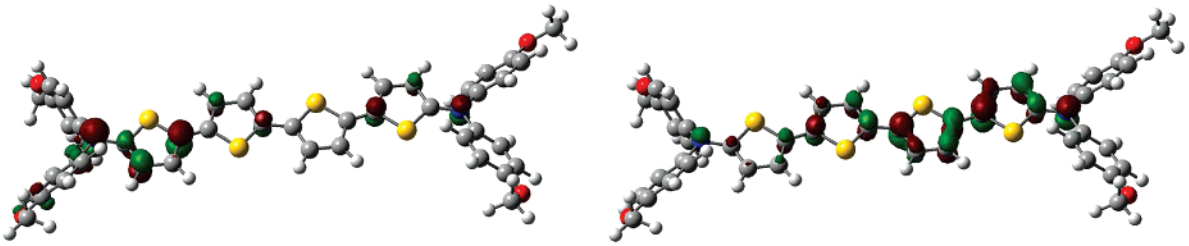

Figure 4. Orbitals (HOMO and SOMO) involved in $(Ar_2N)_24T$ radical-cation first optical transition.

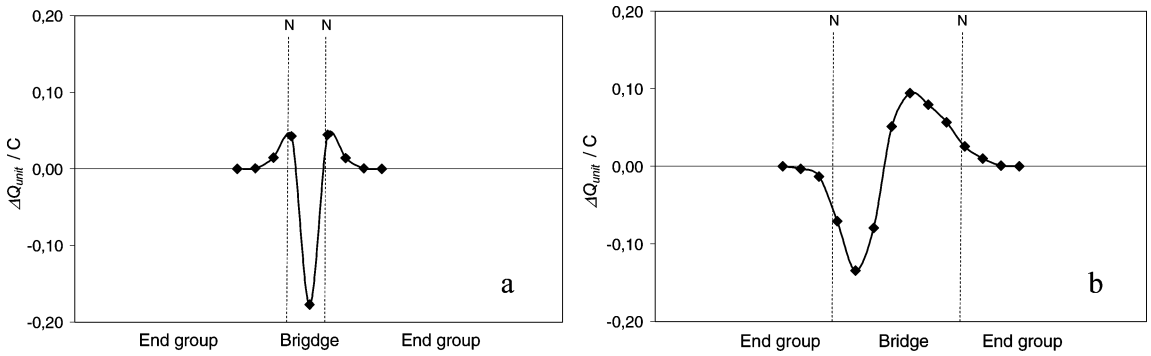

Figure 5. Charge difference between the first excited and the ground states for short (class III) and long (class II) $(Ar_2N)_2nT$ radical cations: (a) $(Ar_2N)_2T$; (b) $(Ar_2N)_26T$.

the weight of configurations involving lower occupied molecular orbitals (i.e., higher excited configurations) increases with the number of thiophene units in the bridge. As these orbitals are localized mainly on the oligothiophene bridge, this can be attributed to the influence of bridge redox state levels on the electron transfer.

Charge Distribution in the First Excited State. Figure 5 shows the charge difference between the first excited and the ground states for short (class III) and long (class II) $(Ar_2N)_2nT$ radical cations. The charge has been compiled on terminal methyl, oxygen atom, phenyl units, N atoms, and thiophene units. In these representations negative values indicate the groups or atoms which gain negative charge upon excitation. It can be seen that the charge distribution in the first compounds remains symmetrical after optical excitation. On the contrary, the charge in the class II compounds is localized on the other part of the molecule, showing that photon absorption is indeed provoking electron transfer from one side of the molecule to the other. However, the simple picture of a single electron transferring from one neutral nitrogen to the oxidized nitrogen is not completely appropriate, since it can be seen that the charge depletion on the former and the charge increase of the latter are much smaller than unity and that the thiophene rings are highly affected in the process. In other words the effective charge-transfer distance is smaller than the N−N distance.

Solvent Effect. It is often assumed that the dielectric continuum theory equation introduced by Marcus is at least semiquantitatively correct for the CT band: $\lambda_{out} = e2\ g(r,d)\ (1/n^2 - 1/\epsilon_s)$, where n is the refractive index, ϵ_s, the static dielectric constant, r, the radius of the charge-bearing units, and d, the charge-transfer distance. The simplest form for $g(r,d)$ is $g(r,d) = (1/r - 1/d)$ and requires that $d > 2r$, which is often not the case, and an ellipsoidal correction to account for the nonspherical shape of real molecules has been employed.[51]

(51) Brunschwig, B. S.; Ehrenson, S.; Sutin, N. *J. Phys. Chem.* **1986**, *90*, 3657.

$(Ar_2N)_2nT$ radical-cation geometries have been optimized at the UAM1SM5C level which models aqueous solvation. PM3-(CI=40)SM5C calculations on the obtained geometries have been run to determine their optical properties. This modeling has not been used in previous studies, and therefore, caution must be exercised in interpreting the results. They are used here qualitatively to see if it is possible to distinguish between class III (no solvent effect on the first optical transition) and class II compounds (solvent effect giving E_{op} increase). Whether this model is good enough to give the λ_{out} experimental value for a given compound is a different question (but note that the calculated solvent effect will be overestimated, since the method integrates solvent electronic polarization which is faster than electron transfer and gives the $(1/n^2 - 1/\epsilon_s)$ terms of the Marcus equation).

For the bisdiarylaminothiophene radical cation, the calculated geometry and charge distribution remain symmetrical. The bond length alternation is reversed, and the N−C_α bond is shorter than that in the neutral molecule (1.36 Å versus 1.41 Å). It is therefore predicted to be a class III compound in solution with $E_{op} = 2H_{ab} > \lambda_{in} + \lambda_{out}$.

For the bisdiarylaminobithiophene radical cation, the calculated geometry and charge distribution are not symmetrical and are consistent with the formation of a localized charge defect characterized by a semiquinoidal structural distortion. This charge is situated on one side of the molecule, and consequently, one of the N−C_α bonds is short. It is therefore predicted to be a class II compound in solution, whereas it appeared to be class III in the gas phase. This result makes us confident in the molecular modeling procedure used, since this localization upon introducing a solvent effect is qualitatively expected.

$(Ar_2N)_2nT$ radical cations with longer bridges have unsymmetrical geometries and remain class II compounds but according to Hush theory should experience the full solvent effect on their CT band, since $E_{op} = \lambda_{in} + \lambda_{out}$, whereas in the gas-phase $E_{op} = \lambda_{in}$.

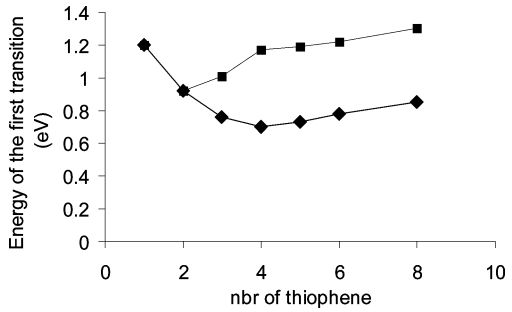

Figure 6. Calculated solvent effect on the energy of the first optical transition in $(Ar_2N)_2$nT radical-cation series: (◆) E_{op} in the gas phase; (■) E_{op} in water.

Calculated solvent effects on CT bands are shown in Figure 6 which compares the energy of the first transition in the gas phase and in aqueous solution.

It appears that for the bisdiarylaminothiophene radical cation the first transition band is solvent-independent, whereas for bisdiarylaminothiophene with 4T, 6T, and 8T bridges a large increase in the E_{op} is predicted. Such results are fully in line with what is expected for class III and class II compounds.

Overall, the results presented in this first part of this paper are not surprising and confirm that $(Ar_2N)_2$nT radical cations are organic mixed valence compounds. A transition between class III and class II compounds is calculated when the number of thiophene units between the two charge-bearing units increases.

Short $(Ar_2N)_2$nT radical cations are class III compounds and have a first, solvent-independent, optical transition not associated with electron transfer and $E_{op} = 2H_{ab}$.

Longer $(Ar_2N)_2$nT radical cations are class II compounds and have a first, solvent-dependent transition associated with electron transfer and $E_{op} = \lambda_{in}$ $(+\lambda_{out}) > 2H_{ab}$. Electron transfer is thermally activated and can be described within the framework of the Hush theory, which makes it possible to extract from the UV−vis−near-IR spectra the intrachain electron transfer constant. However, the simple picture of a single electron transfer from one neutral nitrogen to the oxidized nitrogen is not completely appropriate, since the charge-transfer distance is smaller than the N−N distance and the thiophene rings are highly affected in the process. Furthermore, calculations suggests that, as the number of thiophene units in the bridge increases, charge transfer from the low-lying redox states of the oligothiophene units will start to interfere with charge transfer from the "reduced diarylamino group" to the "oxidized diarylamino group". In other words, electron transfer will switch from a superexchange mechanism to a chemical mechanism for some length of the oligothiophene bridge.

II. Oligothiophenes. We now turn in the second part of this study to oligothiophene radical cations.

Gas-Phase Geometry. Neutral systems have symmetrical geometries with bond length alternation in which the $C_\alpha-C_\beta$ bonds are short, whereas the $C_\beta-C_\beta$ and $C_\alpha-C_{\alpha'}$ bonds are long.

Figure 7 shows the gas-phase bond length alternation of several oligothiophenes in their singly oxidized states. The geometries of the radical cations are bridge-length-dependent.

For short oligothiophene radical cations (Figure 7a) consisting of one to eight thiophene units, the calculated geometries are symmetrical but the bond length alternation is reversed compared to that of the neutral molecule. In a mixed valence description such calculated geometries are indicative of class III compounds with a fully delocalized electron and $2H_{ab} > \lambda$.

For intermediate oligothiophenes the calculated geometries remain apparently symmetrical (Figure 7b), as already reported by several groups, but are also consistent with the formation of a localized charge defect characterized by a semiquinoidal structural distortion. This defect is situated at the center of the oligothiophene (as opposed to localization on one side of the molecule in $(Ar_2N)_2$nT radical cations). This defect extends over several thiophenes and can be estimated to be between five and six thiophene units long, as judged by the bond alternation pattern presented in Figure 7b. This is two to three thiophene units more than the localized charge defect observed in the $(Ar_2N)_2$nT radical-cation series. For more than eight thiophene units the localized charge defect seems similar for all the structures calculated. For longer oligothiophenes, several geometries lying within kT can be obtained (16T: nonsym = 601.253 kcal, sym = 601.249 kcal; 12T: nonsym = 491.833 kcal; sym = 491.832 kcal) depending on the starting geometries of the .dat file. We will focus on unsymmetrical geometries depicted in Figure 7c and 7d for 12T and 15T radical cations because comparison with the results obtained in $(Ar_2N)_2$nT radical-cation series will be easier. The calculated geometries are still consistent with the formation of a localized charge defect characterized by a semiquinoidal structural distortion. However, this defect is now situated on the left side of the oligothiophene (similar to $(Ar_2N)_2$nT radical cations). This defect still extends over five to six thiophene units, appears to be chain-length-independent, and presents the same bond alternation pattern as when the charge defect is on the center of the oligothiophene. It therefore seems that above some length the charged defect can be localized on several (at least three, i.e., left, center, or right side) energetically equivalent sites.

Charge Distribution in Ground State. Figure 8 shows the charge distribution of two oligothiophene radical cations. These charges are compiled on each thiophene unit. This rather empirical description makes it possible to represent qualitatively the extent of charge delocalization on the molecule.

As expected for short and intermediate oligothiophene units (Figure 8a), the calculated charge distribution is symmetrical and is delocalized over the whole molecule, which suggests a class III character for these systems. Furthermore, for these oligomers the defect tends to spread out as the oligomer length increases, but such spreading seems to have a limit, since above 8T the spatial extension remains constant.

For long oligothiophenes such as 16T (Figure 8b) and 22T (Figure 8c) in which the calculated geometry can be unsymmetrical, the charge distribution is obviously no longer symmetrical and is localized on one side of the molecule. The charge defect extends mainly over the first six thiophene units of the oligothiophene and is the same as when it is localized at the center of the molecule. For such oligothiophenes the spatial extension of the charge defect is now oligothiophene-length-independent. In a mixed valence description such calculated geometries and charge distributions are indicative of class II compounds with the appearance of at least two minima in the adiabatic potential surface and an activation barrier separating these minima. Such behavior is fully comparable with what is seen in the $(Ar_2N)_2$nT series, suggesting that when the number of thiophene units increases H_{ab} decreases, and for some

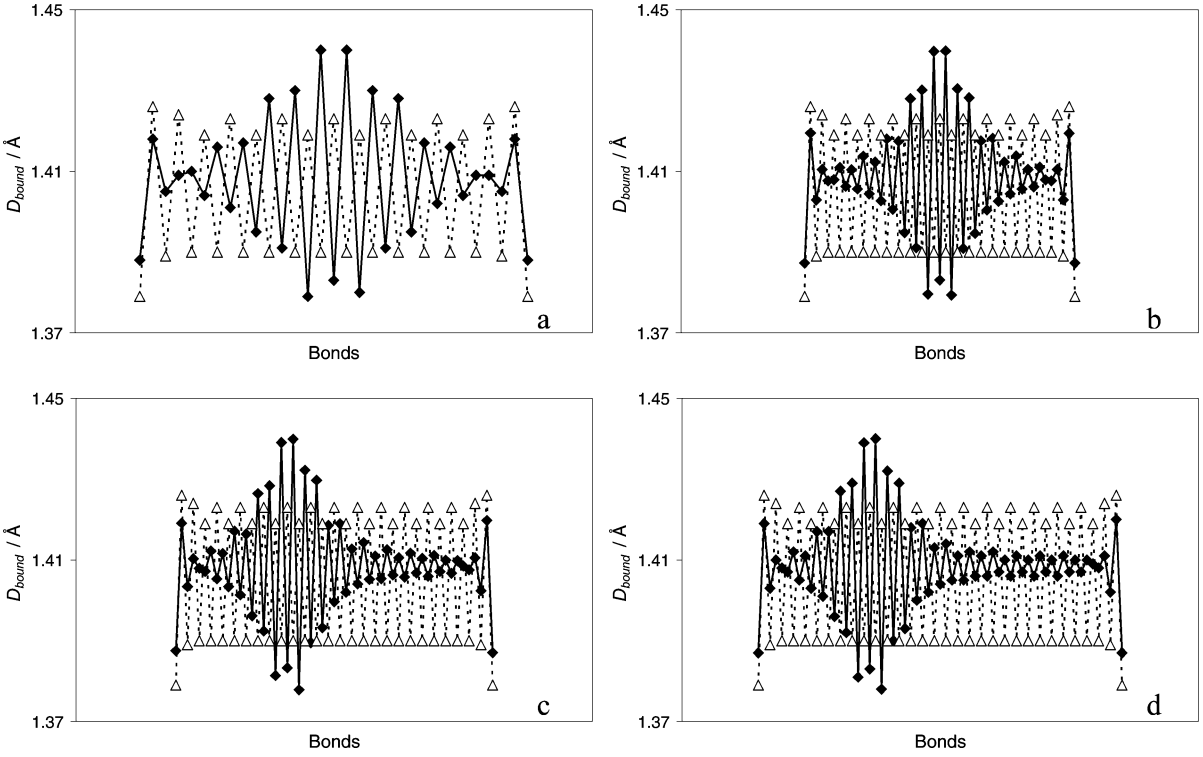

Figure 7. Calculated geometries of neutral (△) and monooxidized (◆) oligothiophenes: (a) 6T; (b) 9T; (c) 12T; (d) 15T. For 12T and 15T radical cations several geometries can be obtained within kT and differ in the location of the geometric deformation. Only unsymmetrical geometries are shown here.

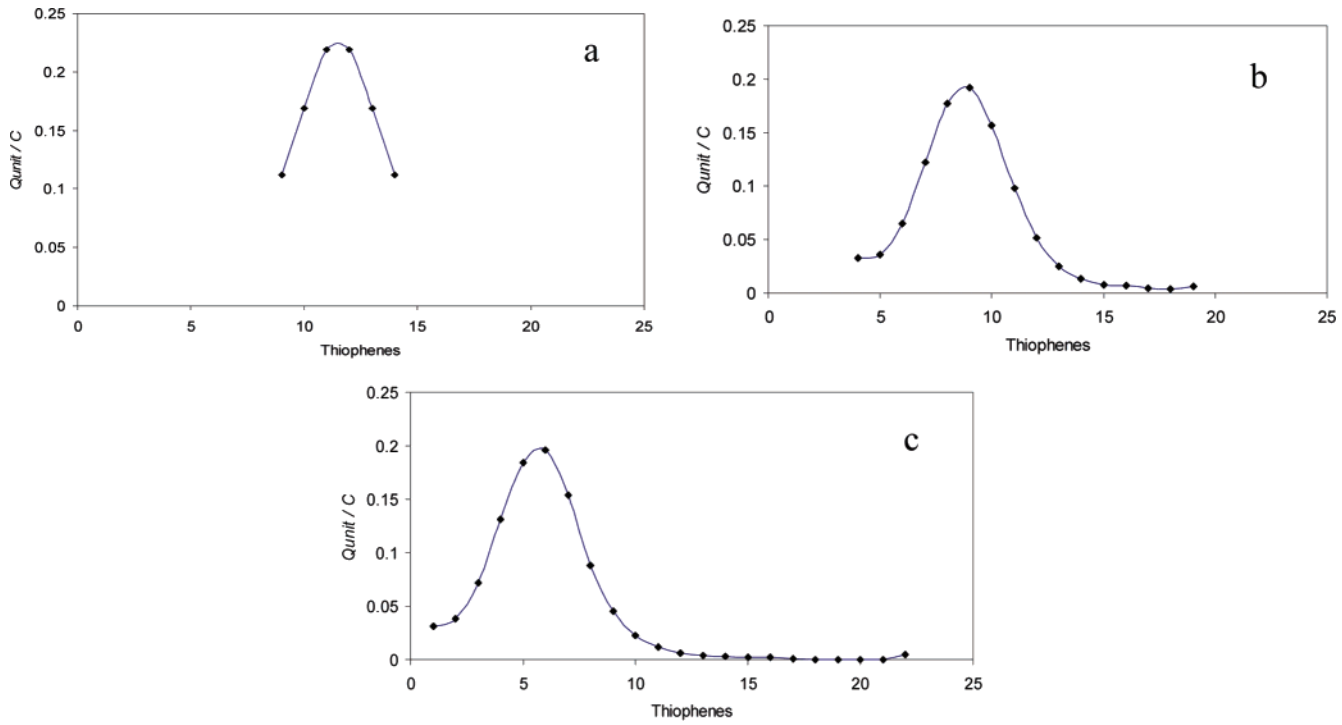

Figure 8. Charge difference between OnT radical cation and neutral OnT: (a) 6T; (b) 16T; (c) 22T.

oligothiophene length $2H_{ab}$ will become lower than λ, giving a transition between class III and class II.

Optical Properties. The UV−vis−near-IR spectra of the molecules have been calculated at the PM3(CI=40)//AM1 and TDDFT (for the first members of the series) levels. Let us recall that good agreement is obtained among PM3(CI=40)//AM1, TDDFT, and experimental E_{op} results (see Table 1).

Table 3 gives the transition energies, intensities, and main CI expansion coefficients of the first excited state for these compounds.

We will first focus on short and intermediate oligothiophenes. The lowest energy transition is at 1.19, 0.88, and 0.727 eV for 3T, 6T, and 8T, respectively, and is associated with an initially low but strongly increasing transition dipole moment (1.1, 8.0,

Table 3. PM3CI//UAM1-Calculated Transition Energies, Oscillator Strength, and Main CI Coefficients in the Excited State for OnT Radical Cations

compound	E_{op} [eV]	oscillator strength	main CI coefficients of the excited state
3T	1.19	0.005	42% HOMO → SOMO 42% SOMO → LUMO
4T	1.00	0.037	51% HOMO → SOMO 36% SOMO → LUMO
6T	0.88	0.213	64% HOMO → SOMO 22% SOMO → LUMO
8T	0.73	0.456	65% HOMO → SOMO 15% SOMO → LUMO
10T	0.67	0.719	62% HOMO → SOMO 10% SOMO → LUMO 15% HOMO − 2 → SOMO
16T	0.63	0.894	4% HOMO → SOMO 25% HOMO-1 → SOMO 38% HOMO-2 → SOMO 17% HOMO-4 → SOMO 7% SOMO → LUMO
22T	0.61	0.861	3% HOMO → SOMO 9% HOMO-1 → SOMO 20% HOMO-2 → SOMO 34% HOMO-3 → SOMO 3% SOMO → LUMO

and 12.9 D, respectively) directed along the long axis of the oligothiophene, indicating that the intensities of these transitions are highly oligomer-length-dependent. These lowest energy absorptions essentially correspond to a transition between the SOMO and the LUMO and between the HOMO and the SOMO, as judged by the main CI coefficients of the excited states. The three orbitals involved in this first transition are delocalized over the whole oligomer, and therefore, such transitions can be seen as $\pi-\pi^*$ transitions and are not associated with a charge-transfer process. Apart from these weak transitions the spectra are dominated by intense bands at 2.12, 1.69, and 1.50 eV, respectively. Like the lowest energy absorption these absorptions correspond to a transition between the SOMO and the LUMO and between the HOMO and the SOMO with reversed main CI expansion coefficients of the excited states.

These results fully agree with the experimental observation of 2T, 3T, and 6T radical-cation spectra published in the literature and are also coherent with the TDDFT calculations performed in this work. Furthermore, these results are very similar to those reported in the first part of this paper on short class III $(Ar_2N)_2$nT radical cations in every detail (number of optical transitions, nature of the orbitals involved in the transition, decreasing E_{op} with increasing oligomer length).

Long oligothiophenes with unsymmetrical charge defects have a first optical transition which is associated with a very strong transition dipole moment directed along the long axis of the oligothiophene (19.5 and an 19.3 D for 16T and 22T, respectively). The E_{op} and transition dipole moments are almost stationary and do not depend on oligomer length. When compared to the results obtained for class II $(Ar_2N)_2$nT radical cations, the results are also very similar (localization of the charged defect on one part of the molecule, strong and stationary transition dipole moments, weight of the higher-excited configurations increasing with the number of thiophene units). Figure 9 displays two molecular orbitals involved in the first transition for the 16T radical cation (SOMO and HOMO-2 orbitals) with a schematic representation of the charge localization in the ground state prior to photon absorption. The SOMO

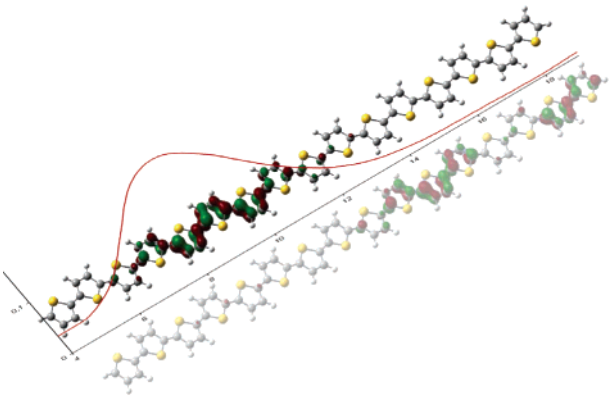

Figure 9. Orbitals involved (HOMO-1 and SOMO) in 16T radical-cation first optical transition with a schematic representation of the charge localization in the ground state prior to photon absorption.

is localized in the part of the molecule bearing the charged defect, whereas the HOMO-1, -2, and -4 orbitals are in the central part of the molecule. This clearly suggests that this transition is associated with charge transfer from the center of the oligomer toward the side of the molecule bearing the charge defect in the ground state.

In a mixed valence description such results are usually considered as indicating that when the oligothiophene is smaller than 8T, the radical cations can be seen as class III compounds and $E_{op} = 2H_{ab}$ suggesting that H_{ab} is 0.6, 0.44, and 0.36 eV for 3T, 6T, and 8T, respectively, whereas, for oligothiophenes longer than 8 to 10T, the radical cations could be considered as class II compounds with $E_{op} = \lambda_{in} > 2H_{ab}$.

Charge Distribution in the First Excited State. Figure 10 compares the charge distribution in the ground state and in the first vertical excited state for oligothiophene radical cations. It can be seen that the charge distribution in short and intermediate oligomers remains symmetrical after optical transition and is not severely affected by photon absorption. For 6T and 8T some charge-transfer character from the side toward the center of the oligomer is observed, but the electronic structure is likely to relax toward the initial distribution, since no space is available to accommodate the polaron on both sides of the molecule. On the contrary, the charge distribution in the first excited states of unsymmetrical 16T and 22T is clearly localized on a different part of the oligomer than in the ground state. Photon absorption in the first absorption band makes it now possible to provoke electron transfer from one part of the molecule to another. Careful examination of the charge distribution in the first vertical excited states strongly suggests that the effective electron-transfer distance is around three thiophene units, i.e., smaller than the spatial extension of the polaron. This suggests that, when the polaron has room to move along the oligomer and is not confined by the size of the quantum box of short oligomers, short intrachain electron transfer occurs. Furthermore, the electron-transfer distance appears to be identical in 16T and 22T radical cations and is thus oligomer-length-independent, which in a mixed valence description means that λ_{in} is also oligomer-length-independent and, since $E_{op} = \lambda_{in}$, explains why E_{op} remains almost constant for long oligothiophenes. This result is important, since many experimental studies have plotted E_{op} versus $1/n$ and observed linear dependence for short oligomers. Extrapolation of these curves has been used systematically for evaluating the optical properties of the polymer.[4a,7,13,17] It is clear

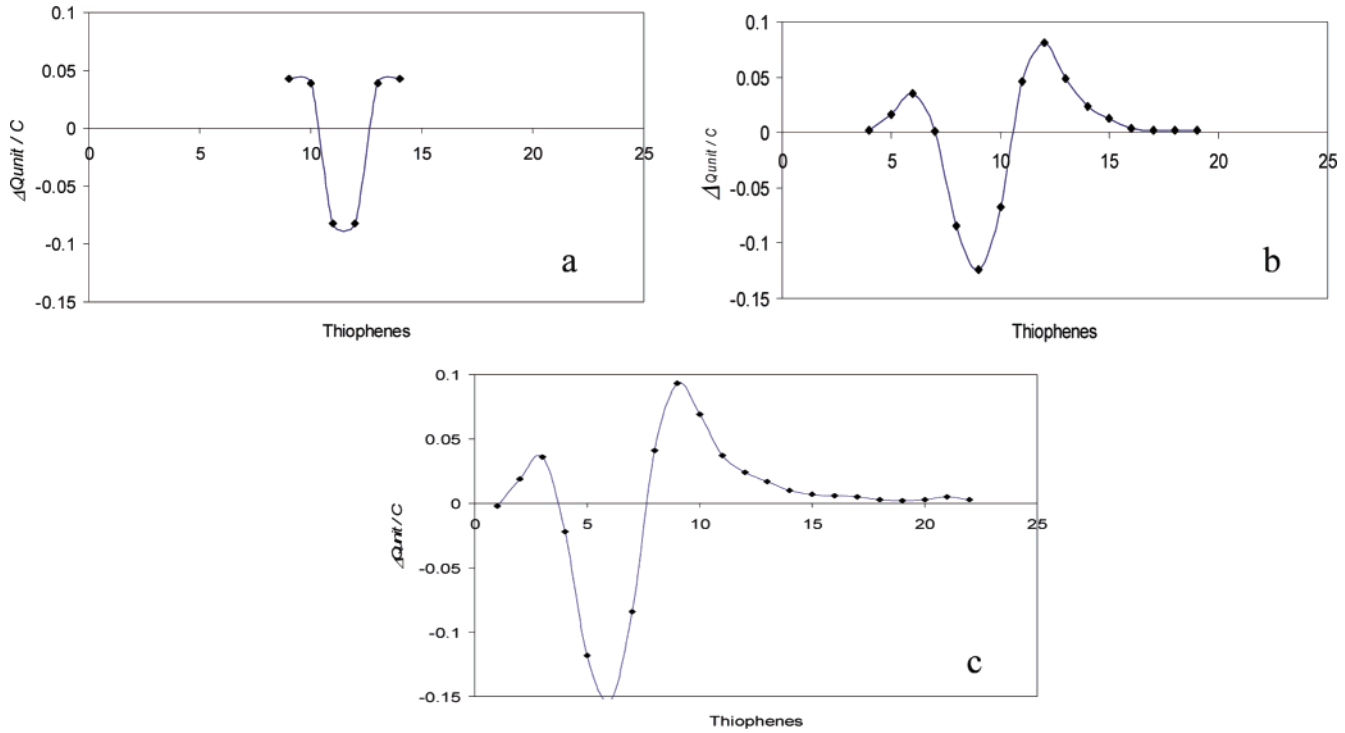

Figure 10. Charge difference between the first excited and the ground states for OnT radical cations: (a) 6T; (c) 16T; (c) 22T.

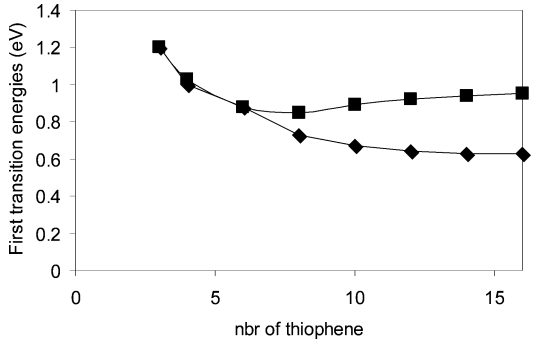

Figure 11. Calculated solvent effect on the energy of the first optical transition in OnT radical-cation series. (◆) E_{op} in the gas phase; (■) E_{op} in water.

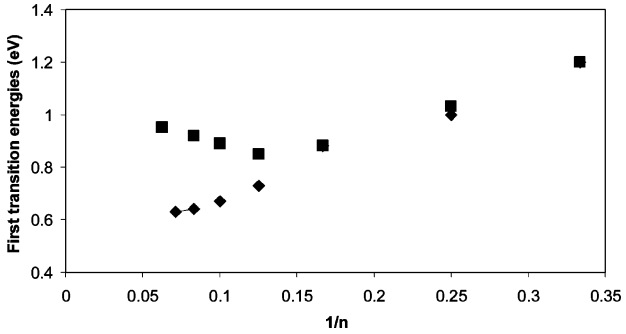

Figure 12. Calculated energy of the first optical transition in OnT radical-cation series versus 1/*n*. (◆) E_{op} in the gas phase; (■) E_{op} in water.

here that when the size of an oligomer exceeds that of the localized charge defect, this linear dependence is no longer observed. However, the E_{op} versus 1/*n* is linear for oligothiophenes shorter than 8−9T.

Solvent Effect. One of the very marked characteristics of mixed valence compounds is solvent effect on the charge-transfer band. Indeed, for class III compounds, the first optical transition is solvent-independent, whereas, for a class II compound, the absorption band maximum shows the full solvent effect.

In the $(Ar_2N)_2$nT radical-cation series, molecular modeling has shown that E_{op} is solvent-independent for a bridge consisting of a single thiophene unit, whereas E_{op} increases when compared to gas-phase results for longer bridges (see Figure 6). Molecular modeling used in this study is therefore capable of qualitatively reproducing this marked difference between class III and class II compounds.

Figure 11 gives the overall evolution of calculated E_{op} versus oligomer length for the oligothiophene radical cations under study in the gas phase (curve a) and in aqueous solution (curve b).

It can be seen that for short and intermediate oligomers the first optical transition is not influenced by the solvent, which is characteristic of class III compounds. On the contrary, solvent effects are predicted (increase in E_{op}) above 8T and indicate a transition between class III and class II compounds. Comparison of Figure 6 and Figure 11 shows that the $(Ar_2N)_2$nT and the OnT radical-cation series exhibit very similar solvent effects. We believe that this last result associated with that of the geometries, ground state charge distribution, optical properties, and the charge distribution in the vertical first excited states is clear theoretical proof of the mixed valence character of slightly doped conductive oligomers and polymers.

As a consequence, Figure 12 shows that it is not possible to extrapolate some of the properties of the doped polymer on the basis of the often reported linearity of these properties versus 1/*n* using short oligomers as model compounds[4a,7,13,17] (where *n* stands for the number of monomer units). Indeed, short oligomers and conducting polymers are not similar in terms of intrachain electron transfer and must be considered to some extent as different materials.

Overall, the results presented in the second part of this paper demonstrate that conducting oligomer radical cations and slightly doped conducting polymers are a special case of organic mixed valence compounds. A transition between class III and class II compounds is predicted when the number of thiophene units exceeds eight to nine in the gas phase, and most probably for shorter oligomers when counterion effects and ion pairing are important.

Short oligomers are class III compounds and have a first, solvent-independent optical transition which is not associated with intramolecular electron transfer and $E_{op} = 2H_{ab}$. This makes it possible to evaluate the decrease in H_{ab} with oligomer length and the fall in electronic coupling as the size of the oligomer increases.

Longer oligomers and, more importantly, conducting polymers are class II compounds have a first, solvent-dependent transition associated with short-range distance electron transfer and $E_{op} = \lambda_{in}$ $(+\lambda_{out}) > 2H_{ab}$. Intrachain electron transfer is thermally activated and can be described within the framework of the Hush theory, which makes it possible to extract from the UV−vis−near-IR spectra the electron-transfer constant along the π-conjugated chain. The electron-transfer distance associated with the first optical transition is short (three thiophene units) and oligomer-length-independent. λ_{in} can be quantitatively evaluated from gas-phase results and is found to be 0.62 eV, whereas λ_{out} can be estimated qualitativaly to be around 0.3 eV (recall that overestimation is most probable because solvant polarization is taken into account in the modeling). Note also that λ_{out} in acetonitrile or in the solid phase will most probably be smaller, whereas counterion and ion-pairing effects will increase λ_{out} and will affect the delocalization(classIII)/localization(classII) transition in terms of oligomer length.

III. Experimental Evidence of Oligothiophene Radical-Cation Mixed Valence Properties. The inorganic and organic mixed valence scientific community uses several experimental criteria to determine the class of the compounds under study, to characterize the localization/delocalized transition, and to extract from the optical properties the pertinent parameters for intramolecular electron transfer characteristics. We will not use all of them but will only focus on time scales and band truncature.

Any dynamic system can be studied by different techniques, each characterized by its own time scale. Typical time scales are $1-10^{-5}$ s for ^{1}H NMR, $10^{-5}-10^{-9}$ s for EPR, and $10^{-11}-10^{-12}$ s for IR, 10^{-13} s for solvent response to changes in the local electric field, 10^{-14} for vis−near-IR CT transitons, and 10^{-17} s for solid-phase XPS spectroscopy. If intramolecular electron transfer is sufficiently rapid on these time scales, only averaged signals will be observed in a given case. The combined use of several probes with different time scales makes it possible to estimate quite precisely the order of magnitude of the electron-transfer constant.

For example, Nelsen et al.[31,41,52] have extensively studied bis(hydrazine) compounds with saturated or aromatic bridges by means of EPR spectroscopy. Such compounds exhibit important reorganization energies which makes the electron transfer time constant close to the EPR time scale. Using temperature to modulate electron transfer and fine structure coalescence in the EPR signal they have measured precisely k_{et} and have challenged SET theories. Other groups have used IR line broadening and coalescence or an IR marker, such as symmetrical bridging ligand stretches, for estimation of k_{et} for faster electron transfer (differences in the response of different types of vibrational mode have also been used).[24,53] Two sets of Ru_{3p} ionization energies are observed in some inorganic MV compounds, suggesting localization on the XPS time scale, whereas other examples have been published in which only a single set of XPS binding energies is observed.[24,54]

Of course, the shape of the CT bands provides the most systematic marker for localization and class II (broad, solvent-dependent band), class III (narrow, solvent-independent band) behavior but a new class II−III has been recently introduced for borderline systems. Extensive work has been published on this class II−III, and optical transitions of symmetrical mixed-valence systems in this transition regime have been reviewed.[24,32,36] For such "almost delocalized" systems the new feature is the cutoff of the CT band on the low-energy side when H_{ab} approaches the reorganization energy. Band shape analysis has become a powerful tool to analyze such systems.

When looking through the abundant literature concerning oligothiophene radical-cation characterization, several experimental observations can be reanalyzed in the light of the above ideas.

Let us first focus on EPR spectroscopy. Janssen et al.[4] have published EPR spectra of didodecylsexithiophene (6T), tridodecylnonathiophene (9T), and tetradodecyl duodecithiophene (12T) radical cations. While the first shows a hyperfine coupling pattern, indicating that intramolecular electron transfer if any is slow on the EPR time scale, the latter two do not show any resolvable hyperfine coupling, indicating that intramolecular electron transfer occurs and is fast on the EPR time scale. These results strongly suggest that, under the experimental conditions of Janssen's study, 6T is a fully delocalized class III compound, whereas 9T and 12T are class II−III or class II compounds with fast ($k_{et} > 10^9$ s^{-1}) but thermally activated intramolecular electron transfer.

The first optical transition reported for these species is at 0.84, 0.67, and 0.59 eV for 6T, 9T, and 12T, respectively,[4] close to the calculated values reported in this study (0.88, 0.69, and 0.62 eV, respectively). Turning now to the shape of these bands (see Figure in ref 4), one can notice that the band for 6T is narrow and shows the beginning of a vibronic progression on the high-energy side, whereas for 9T and 12T band broadening occurs. A cutoff of the band on the low energy side is clearly visible for 6T and 9T radical cations, whereas for the 12T radical cation the cutoff is much less pronounced. We believe that these results associated with the EPR observations can be reinterpreted as a

(52) (a) Nelsen, S. F.; Ismagilov, R. F.; Powell, D. R. *J. Am. Chem. Soc.* **1997**, *119*, 10213. (b) Nelsen, S. F.; Ismagilov, R. F.; Gentile, K. E.; Powell, D. R. *J. Am. Chem. Soc.* **1999**, *121*, 7108. (c) Nelsen, S. F.; Ramm, M. T.; Wolff, J. J.; Powell, D. R. *J. Am. Chem. Soc.* **1997**, *119*, 6863.

(53) (a) DeRosa, M. C.; White, C. A.; Evans, C. E. B.; Crutchley, R. J. *J. Am. Chem. Soc.* **2001**, *123*, 1396. (b) Ito, T.; Hamaguchi, T.; Nagino, H.; Yamaguchi, T.; Kido, H.; Zavarine, I. S.; Richmond, T.; Washington, J.; Kubiac, C. P. *J. Am. Chem. Soc.* **1999**, *121*, 4625. (c) Demadis, K. D.; Neyhart, G. A.; Kober, E. M.; Meyer, T. J. *J. Am. Chem. Soc.* **1998**, *120*, 7121. (d) Wu, R.; Koske, S. K.; White, R. P.; Anson, C. E.; Jayasooriya, U. A.; Cannon, R. D.; Nakamoto, T.; Katada, M.; Sano, H. *Inorg. Chem.* **1998**, *37*, 1913.

(54) (a) Citrin, P. H. *J. Am. Chem. Soc.* **1973**, *95*, 6472. (b) Lazarus, M. S.; Sham, T. K. *J. Am. Chem. Soc.* **1979**, *101*, 7622. (c) Spreer, L. O.; Allan, C. B.; MacQueen, D. B.; Otvos, J. W.; Calvis, M. *J. Am. Chem. Soc.* **1994**, *116*, 2187.

transition between class III (6T radical cations) or class II (9T and 12 T radical cation) mixed valence compounds and that the intramolecular electron-transfer rate can be derived from the usual Hush treament of the CT band.

Band shapes and solvent effects for short oligothiophene radical cations ($n < 9$) generated by pulse radiolysis have been reported.[11] The band shape and minimal solvent effect observed are strong indications of class III behavior for these oligomers. On the contrary, the bands associated with doped polythiophene (and more generally conducting polymers) are broad and unresolved, suggesting class II behavior, even though the juxtaposition of bands associated with oligomers of various lengths can also be at the origin of such broadening. Moreover, Lambert and Nöll[55] have recently polymerized bis(triarylamine) systems with conjugated bridges, and the polymers show on one hand an electroactive behavior quite similar to that of a conductive polymer and on the other hand broad and intense intervalence charge-transfer bands quite similar to those in the monomeric MV model compounds.

Other experimental evidence for mixed valence properties of conducting polymers can be found in the many XPS studies that have been published.[56] Indeed, polypyrrole, polythiophene, and polyaniline when in their oxidized states have N or S XPS signals that do not show a single peak as would be the case for class III compounds, but several peaks which have been attributed to "neutral nitrogen or sulfur atoms" and "oxidized nitrogen or sulfur atoms", the ratio between these two signals being used to evaluate the doping levels of the polymers. This could be taken as evidence for localization on the XPS time scale and of class II character. We are not aware of XPS studies on short class III oligomer radical cations.

Raman spectral bands have been attributed to two separate forms of the polymers, i.e., the oxidized forms and the reduced forms of the chains.[57] Even though such studies have not been performed with the idea that coalescence could occur for very fast electron transfer, this finding implies that localization occurs on the Raman time scale for conducting polymers and points toward class II behavior for material consisting of long chains.

Finally, mobilities of charge carriers between π-conjugated polymer chains have been studied on poly[3′,3″,4‴,4⁗-tetrahexyl-sexithiophen-5,5⁗′-diyl)ethylene] (PSE) where sexithiophene units are separated by insulating ethylene units limiting intrachain π-electron transfer.[58] The results show absorption bands at 0.85 and 1.65 eV attributed to the sexithiophene radical cation for low doping levels and a corresponding mobility of 10^{-6} cm^2 V^{-1} s^{-1}, in close agreement with mobilities in polythiophene, whereas at higher doping levels two absorption bands at 0.90 and 1.80 eV dominate the spectra. They are attributed to the formation of π-dimers between two sexithiophene radical cations and coincide with a decrease in the measured charge-carrier mobility. These results have been interpreted as indicating that intrachain hopping of charges in polythiophene film may contribute little to macroscopically observed conductivities. It also strongly suggests that molecular materials with high mobility will be achieved not by extending the π-conjugation length of a polymer but by enhancing a $\pi-\pi$ interaction between π-conjugated units. Furthermore, on the basis of the mobility decrease when π-dimers are generated, it was suggested that π-dimers do not contribute to interchain electron transfer and that a hopping transport of charges is unlikely to be mediated by such species. Analyzing these results within the scope of the present studies leads to the same conclusions. Intrachain hoppings in PSE are slow because they involve SET between two charge-bearing units separated by aliphatic units. A class I or class II situation with a small H_{ab} similar to that in bishydrazine or bisaminophenyl separated by a saturated bridge. Turning to interchain electron transfer, π-dimers are equivalent to Ru (III)−Ru (III) compounds in which electron transfer does not occur. An effective interchain hopping path will occur through self-exchange SET between one sexithiophene radical cation and one neutral sexithiophene which is equivalent to throughspace single electron transfer in Ru(II)−Ru(III) or hydrazine systems. Such throughspace SET will involve small H_{ab} and will give an activation energy for SET, $\Delta G^{\ddagger}$, close to $\lambda/4$. We believe that interchain self-exchange electron transfer rate constants can be determined indirectly by using the findings on intrachain electron transfer obtained in the present studies and the qualitative determination of λ in conducting oligomers.

Conclusion

Conducting oligomer radical cations and slightly doped conducting polymers are special cases of organic mixed valence compounds.

Short oligomers are class III compounds and have a first, solvent-independent optical transition, which is not associated with intramolecular electron transfer and $E_{op} = 2H_{ab}$.

Longer oligomers and, more importantly, conducting polymers are class II compounds and have a first, solvent-dependent transition associated with electron transfer and $E_{op} = \lambda_{in} (+\lambda_{out}) > 2H_{ab}$.

A transition between class III and class II compounds is predicted when the number of monomer units increases. Oligomers with a well defined conjugation length, which have been extensively used as model compounds for polymers, are therefore not as appropriate as initially thought, since they miss this class III−class II transition. Conducting polymers and materials consisting of short oligomers have distinct properties in terms of intrachain electron transfer and need to be treated as different materials.

Single electron transfer theories can be used when studying interchain and intrachain electron transfer in slightly doped conducting polymers and in materials consisting of short oligomers. The main differences between inorganic, organic, and conducting oligomer or polymer mixed valence compounds lies in the H_{ab} and λ values associated with these different series. Inorganic mixed valence compounds (small H_{ab} and λ); organic

(55) Lambert, C.; Nöll, G. *Synth. Met.* **2003**, *139*, 57.
(56) (a) Chan, H. S. O.; Ng, S. C.; Sim, W. S.; Seow, S. H.; Tan, K. L.; Tan, B. T. G. *Macromolecules* **1993**, *26*, 144. (b) Salaneeck, W. R.; Lundström, I.; Hjertberg, T.; Buke, C. B.; Conwell, E.; Paton, A.; MacDiarmid, A. G.; Somarisi, N. L. D.; Huang, W. S.; Richter, A. F. *Synth. Met.* **1987**, *17*, 291. (c) Camalet, J. L.; Lacroix, J. C.; Aeiyach, S.; Chane-Ching, K. I.; Lacaze, P. C. *Synth. Met.* **1998**, *93*, 133.
(57) (a) Bazzaoui, E. A.; Levi, G.; Aeiyach, S.; Aubard, J.; Marsault, J. P.; Lacaze, P. C. *J. Phys. Chem.* **1995**, *99*, 6628. (b) Bazzaoui, E. A.; Bazzaoui M.; Aubard, J.; Lomas, J. S.; Felidj, N.; Levi, G. *Synth. Met.* **2001**, *123*, 299. (c) Bukowska, J.; Jackowska, K. *Synth. Met.* **1990**, *35*, 143. (d) Holze, R. *Synth. Met.* **1991**, *40*, 379. (e) Poussigue, G.; Benoit, C.; Sauvajol, J. L.; Lere-Parte, J. P.; Chorro, C. *J. Chim. Phys.* **1992**, *89*, 1091. (f) Louarn, G.; Mevellec, J. Y.; Buisson, J. P.; Lefrant, S. *J. Chim. Phys.* **1992**, *89*, 987.
(58) Jiang, X.; Harima, Y.; Zhu, L.; Kunugi, Y.; Yamashita, K.; Sakamoto, M.-A.; Sato, M.-A. *J. Mater. Chem.* **2001**, *11*, 3043.

mixed valence compounds (large H_{ab}, large λ) and conducting oligomers and polymers (large H_{ab}, small λ) are materials in which electron transfer can be described within the same theoretical framework. This induces charge delocalization to occur for systems larger than those for inorganic and nitrogen-centered organic mixed valence compounds.

We believe that the findings of this work will prove useful for the understanding and the design of plastic electronic and molecular electronic devices.

Acknowledgment. We thank the ACI nanosciences program for financial support of this work as well as Dr. J. Lomas for revising our text and correcting the English.

Supporting Information Available: Absolute energies and optimized geometries of all the calculated structures, complete ref 50. This material is available free of charge via the Internet at http://pubs.acs.org.

JA060390A